High-precision deformation and damage development assessment of composite materials by high-speed camera, high-frequency impulse and digital image correlation techniques

Sebastian Myslicki, Markus Ortlieb, Gerrit Frieling and Frank Walther, Dortmund, Germany

Although composite materials like wood, vulcanized fiber and carbon reinforced plastic (CFRP) are already investigated by means of their mechanical properties, the abrupt fracture mechanism as well as the deformation behavior right before and after fracture has not been investigated. However, it is marginally investigated for CFRP because of the quite high fracture speed. The knowledge about the damage evolution as the crack start and propagation can help to improve the strength and sensitivity to fracture by improving the materials structure and to utilize these materials for structural applications. For the investigated materials, fracture happens abruptly as it is the nature of composites and the detailed fracture mechanisms could not be detected by conventional measurement techniques. Therefore, an innovative combination of testing devices is presented which is able to fill this gap. Tensile tests were performed to receive conventional stress-strain curves. At the fracture stage, a high-speed camera recorded the fracture process. This information could be combined with digital image correlation (DIC) to visualize the deformation behavior. At the same time acoustic emission (AE) was used to detect the spectrum of mechanical vibrations which gives information about the released energy due to fracture. The challenging triggering of the high-speed camera was solved for each material individually. By using improved light sources, the recording speed could be set up to 2 million frames per second (Mfps). The investigations show different fracture mechanisms for each composite. Wood and vulcanized fiber were also investigated in different directions due to their anisotropy.

Article Information

Correspondence Address
Sebastian Myslicki
Department of Materials Test Engineering (WPT)
TU Dortmund University
Baroper Str. 303, D-44227 Dortmund, Germany
E-mail: sebastian.myslicki@tu-dortmund.de

Keywords
High-speed camera, digital image correlation (DIC), high-frequency impulse measurement (HFIM), acoustic emission, deformation and fracture mechanisms, tensile tests

Clarifying the details of the fracture process is extremely important for the construction of damage analysis models. The composites tested in this work show a quick fracture process which must be investigated with high-speed imaging technique.

Wood is the oldest construction material but was neglected for a long time in modern constructions. It is experiencing renaissance again because of its lightweight potential, good CO_2 emissions balance, low manufacturing and transportation energy and potential to recycle. Therefore research is going on to reveal the potential that wood also in combination with technical textiles, polymers or metal foils may be used in automobile industry as a replacement or supplement to aluminum, magnesium or CFRP [1]. In future, crash properties of such materials must be characterized as well. So wood fracture behavior is considered in this work.

Vulcanized fiber is based on natural fibers that are formed by parchmentizing to coil-shaped solid material. It is used as a construction material, e. g., for helmets or thermoforming products. Vulcanized fiber might be an eco-friendly replacement for

oil-based polymers in the future. Nevertheless, this natural composite is not well characterized. By Penning et al. [2], the latest characterization work is presented where also a high-speed camera was used to detect crack propagation process. With a recording speed of 0.5 million frames per second (Mfps), a crack propagation perpendicular to the load direction on flat specimens (0.8 mm thickness) that moves from one edge to another could be detected. Thicker material or the anisotropy was not considered.

CFRP is practicable for lightweight constructions in aerospace, automobile and marine as it is light, strong and tough. Damage in composite structures is generally a combination of matrix cracking, fiber breakage and delamination [3]. Nevertheless, fracture models are actually based just on numerical methods [4]. In the development of composite materials, it is becoming increasingly necessary to assess impact strength and the breakage progression process to ensure dynamic safety. Tensile tests in combination with a high-speed camera on a zero-degree unidirectional CFRP (CFRP-UD) with 5 Mfps show that fracture happens from one edge to the other edge by longitudinal crack propagation [4-6]. As triggering glued aluminum foils as part of an electrical circuit were used where fracture leads to open contact. DIC was also used to visualize the deformation behavior. With recording speed of 1 Mfps, the crack speed could be estimated to 1,000 m/s. Two crack propagations, first horizontal then splitting along the fiber, were observed.

A combination of DIC and high-speed camera has been used to investigate metals at high strain rates in uniaxial tests [7], by Split Hopkinson bar methods [8] or by 3-point bending methods to receive the stress intensity factor on a brittle metallic composite [9]. In these investigations 0.05 Mfps was the fastest recording speed.

Besides high-speed camera, also high-frequency impulse measurement (HFIM) is a quick measurement method that is based on mechanical vibrations to help getting information about the fracture process as it could be already shown for CFRP in tensile and fatigue tests [10].

Testing strategy

An innovative combination of ultra-high speed camera, digital image correlation (DIC) and high-frequency impulse measurement (HFIM) for fracture investigations on composites with quick fracture process is presented in the following. First, each measurement technique is presented individually followed by the combination of the overall setup including triggering.

Ultra-high speed camera. Several ultra-high speed camera systems are available on the market, but reaching a certain speed range, all camera systems are facing the same challenge. When light hits the photo diode of the camera, it is almost instantly converted into an electric charge. However, the signal processing, the conversion from an analog electric charge to an appropriate digital signal needs more time and turns out as the bottle neck of the recording process.

To overcome this problem, different kinds of approaches are realized in current camera systems available on the market. One possibility is to build a camera containing several individual sensors and reading out the sensors in a fast sequence. Another possibility is to use special sensor architectures with multiple read-out channels. However, in addition, it is sometimes needed to reduce the effective resolution of a sensor when recording speed is increased allowing the processing unit to handle the data amount in time.

In the performed tests an ultra-high speed camera type HPV-X (Shimadzu) using another working principle is used. The FTCMOS sensor of this camera is equipped with an in-situ storage which allows maximum recording speeds of up to 10 Mfps without a loss of resolution. Using this design during a recording, the analog information is shifted within the sensor into a storage area. This transfer can be realized in a quite fast way. After the recording is finished, the time consuming read out process takes place.

Figure 1 shows the FTCMOS sensor schematically. It can be seen that the sensor consists of one pixel area and two memory areas; one located above and one below the pixel area.

The resolution is fixed to 400 × 250 px, independent of recording speed (10 Mfps interpolated), the maximum recording length is 256 images. The camera can be triggered to each frame, pre- and post-trigger functionality is available.

Digital image correlation (DIC). Digital image correlation (DIC) is able to measure displacements and strain fields on the whole surfaces by an optical-numerical process. The working principle is that an applied speckle pattern is optically measured in initial and deformed state (see Figure 2).

By a correlation of these two pattern states, the displacement field can be calculated. The procedure for that is to match two images to get the displacement fields u(x,y) and v(x,y). Mathematically, the cross-correlation coefficient is used and local regions from the images are compared as shown in Equation (1):

see Equation 1 (1)

Equation 1

$$C(u,v)=\frac{\sum_{i=1}^{m}\sum_{j=1}^{m}[f(x_i,y_i)-\overline{f}][g(x_i',y_i')-\overline{g}]}{\sqrt{\sum_{i=1}^{m}\sum_{j=1}^{m}[f(x_i,y_i)-\overline{f}]^2}\sqrt{\sum_{i=1}^{m}[g(x_i',y_i')-\overline{g}]^2}}$$

with

$$x' = x + u_0 + \frac{\partial u}{\partial x}dx + \frac{\partial u}{\partial y}dy$$

$$y' = y + v_0 + \frac{\partial v}{\partial x}dx + \frac{\partial v}{\partial y}dy$$

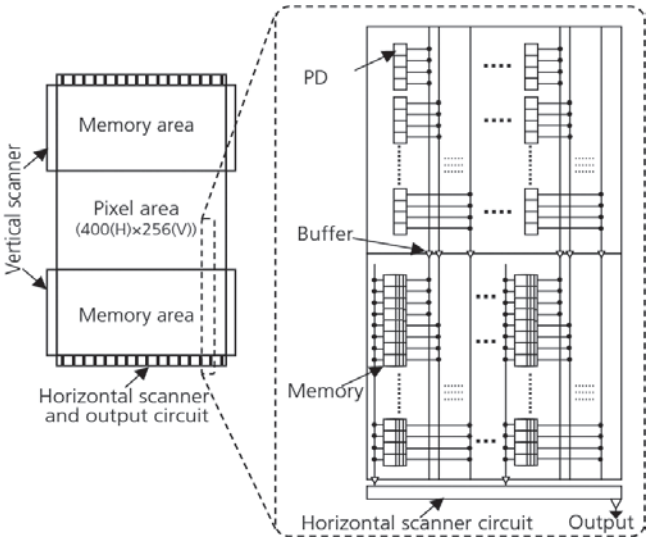

Figure 1: Schematic principle of the FTCMOS sensor for high-speed imaging

In Equation (1), $\bar{f}$ and $\bar{g}$ are the mean intensity values of the reference subset and the deformed subset. u_0 and v_0 describe the translations of the center of the sub-image in x- and y-direction [3].

Using one camera is sufficient for 2D strain measurements in plane regions. Two cameras are needed for 3D strain field calculation. For strain measurements on the surface of flat specimens, only one high-speed camera was used with subsequent DIC calculation on a conventional system type Q400 (Limess).

High-frequency impulse measurement (HFIM). Due to the energy release of fracture from the pre-stressed materials, mechanical vibrations are sending high-frequency impulses through the specimens and attached components. They can be measured by piezo-electrical sensors and transformed into electrical signals. Innovative measurement technique is making use of a real-time process measurement of these impulses and converting them into a three-dimensional landscape consisting of time, frequency and amplitude. Figure 3 shows, e. g., a function (saw-tooth waveform) that is composed of different sine functions with different amplitudes (indicated by a line). Therefore, vibrations could be expressed as function of time f(t) or function of frequency f(ω).

The applied measurement device (type Optimizer4D (Qass)) operates with a sample rate of 3 MHz which makes it possible to detect events within the range of micro-seconds. The measurement device decomposes the time signal into frequency and amplitude based on discrete Fourier transformation (DFT). For efficient computation, the system uses the fast Fourier transformation (FFT) algorithm which allows it to reduce the number of necessary operations significantly and works much more rapidly.

Combination of aforementioned measurement techniques for tensile test application. Quasistatic tensile tests were performed on a universal testing system type AG-X (Shimadzu) with a load cell of 100 kN. The strain was measured by a video extensometer type TRViewX (Shimadzu). The strain rate for all tests was $\dot{\varepsilon} = 3.3 \times 10^{-3}\ s^{-1}$. Specimens were stored and tested under laboratory conditions at 22 °C and 50 % relative humidity prior to testing. The high-speed camera requires a high intensity and highly constant illumination of the test specimens. Therefore, two 400 W (type 400, Arrilux) and three 250 W spotlights (type 25DX, Hedler) with a total light intensity of 34,600 lx were used. Due to the high light intensity, the lense of the video extensometer had to be covered with a filter to ensure an accurate detection of the extensometer marks applied on the specimens. The spotlights and the high-speed camera were mounted on an external frame for an optimal utilization of the working space of the testing machines (see Figure 4a).

The markers for the strain measurement were fixed with 50 mm spacing on the surface of the specimen. Additionally, a microphone and electrical contacts were applied for triggering purpose as well as a piezo sensor for HFIM measurement was applied on the clamping device in low distance to the specimen to ensure an optimal transmission of the mechanical vibrations (see Figure 4b).

The high illuminance generates thermal radiation that heats up the specimens, so that a measurement at constant temperatures was impossible. Therefore, some tests were performed to find an accurate

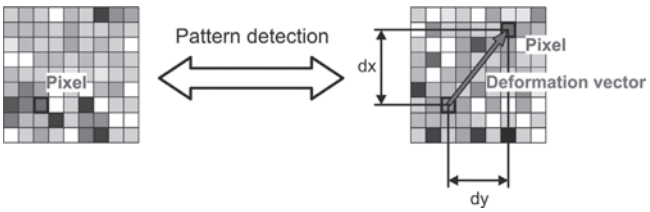

Figure 2: Schematic principle of the deformation measurement by gray scale correlation

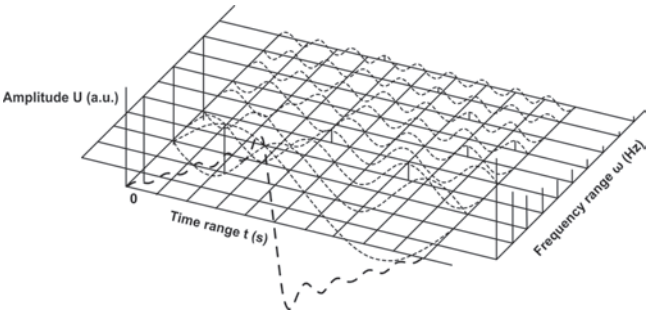

Figure 3: Signal in time and frequency range with course of time t, amplitude U and frequency ω [11]

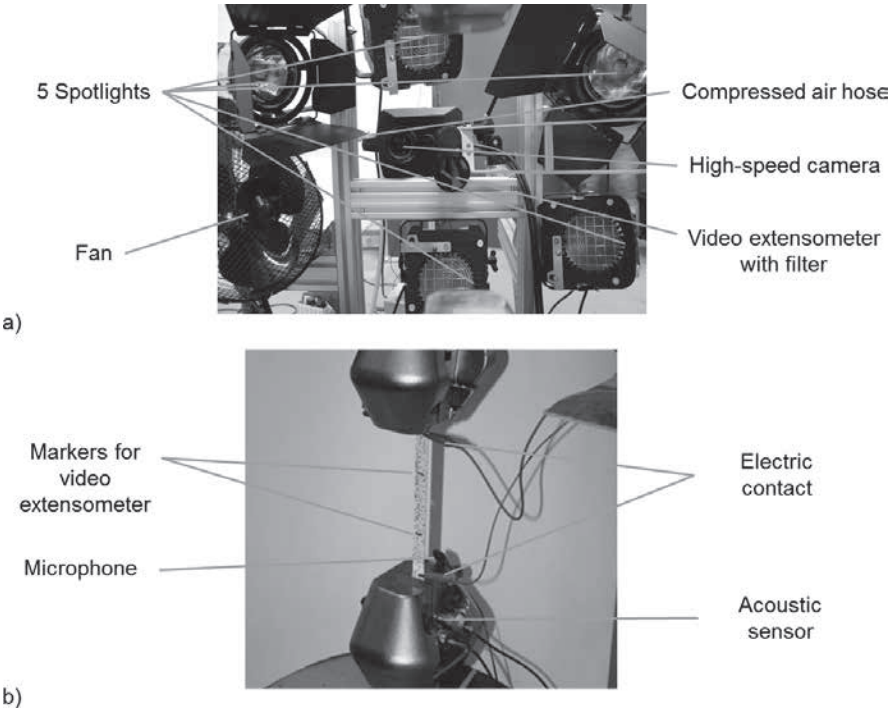

Figure 4: Experimental test setup, a) external frame with high-speed camera, video extensometer and spotlights, b) clamped CFRP specimen with markers for strain measurement, microphone and electrical contacts for triggering and HFIM sensor

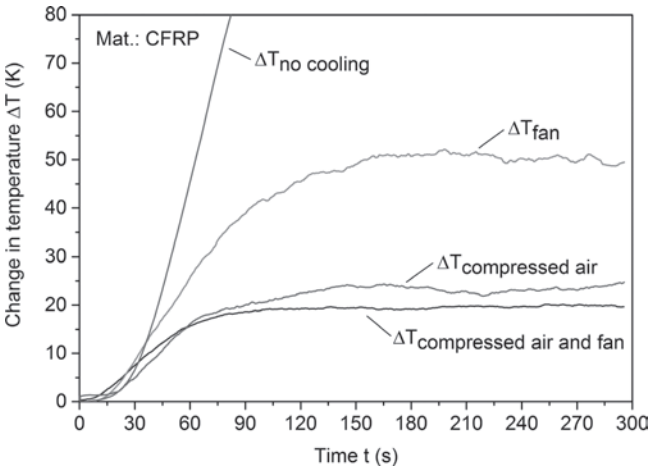

Figure 5: Temperature development for different cooling strategies

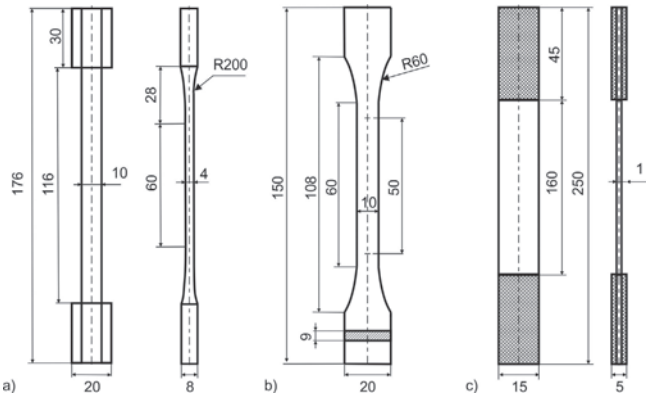

Figure 6: Specimen geometry, a) wood (DIN 52 188), b) vulcanized fiber (DIN EN ISO 527-2:2012), c) CFRP (DIN EN ISO 527-4:1997, type 3)

cooling system. Figure 5 presents the results of the different cooling strategies in form of a diagram where the change in temperature, measured with a thermocouple applied on a CFRP specimen, is plotted against the time.

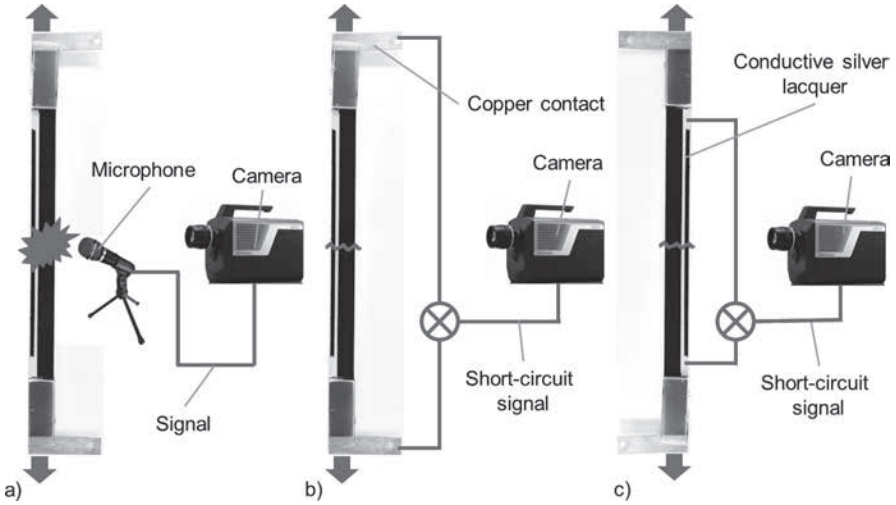

Figure 7: Triggering strategies on CFRP, a) acoustic with microphone, b) electrical with copper contacts on carbon fibers, c) electrical with conductive silver lacquer

Without cooling, the temperature increases in the first 30 s exponentially and afterwards approx. linear. The test was terminated after a temperature change of 80 K. With a conventional fan, the temperature increase reached a plateau at 52 ± 3 K after 150 s. The temperature increase could be further decreased to 24 ± 2 K using a compressed air hose. By using the fan and the compressed air hose simultaneously, the temperature change could be reduced to 20 ± 1 K. Due to the lowest spread of temperature, the last cooling strategy was adopted during the experiments.

In preparation of the experiment, also flash light illumination was an option. However, flash lights need time to get full light intensity. This makes it necessary to get from the experiment a reproducible/reliable signal before the material breaks to trigger the flash light source in advance. With continuous light sources, the timing issue was overcome as observed using flash lights.

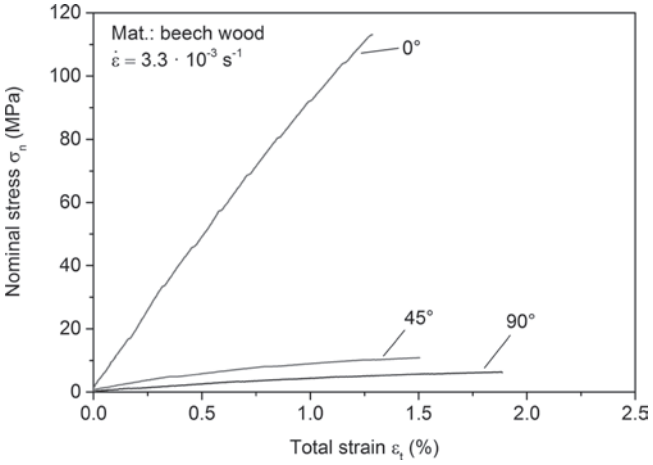

Figure 8: Nominal stress-total strain diagram of beech wood in 0°, 45° and 90° fiber orientation

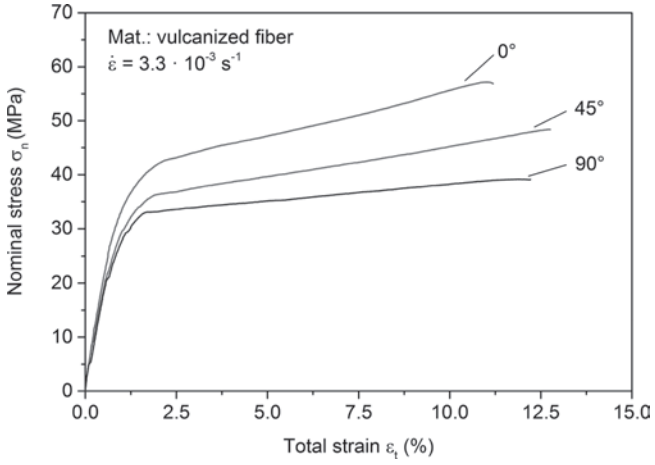

Figure 9: Nominal stress-total strain diagram of vulcanized fiber in 0°, 45° and 90° rolling direction

Specimen preparation and triggering

The wood species used was beech (fagus sylvatica) cut from high-quality defect-free boards. The specimen geometry was dog-bone shaped according to DIN 52 188 (see Figure 6a). The angle of the specimen with regard to the wood grain was set to 0°, 45° and 90°. Dog-bone shaped specimens according to DIN EN ISO 527-2:2012 were cut off from plates of vulcanized fiber with a thickness of t = 9 mm in 0°, 45° and 90° of the rolling direction from the manufacturing process (see Figure 6b). The CFRP specimens were cut off from carbon fiber epoxy prepregs (HS150 EE24 REM) assembled to six layer unidirectional CFRP which was prepared with fiber-reinforced polymer edge bands for an accurate load transmission according to DIN EN ISO 527-4:1997, type 3 (see Figure 6c). Tensile tests were performed only in fiber direction.

On all specimens, a speckle pattern was applied before testing using DIC. Additionally, when applying the pattern, the fracture behavior captured by the high-speed camera becomes more clear. To capture the moment of fracture with high-speed imaging, an accurate triggering is necessary. In the case of wood and vulcanized fiber, the fracture speed is in a range that a microphone, which notices the breakage noise, can be used. Due to the finite speed of sound, the triggering delay is optimized by varying the distance of the microphone to the fracture localization. The fracture speed of CFRP is too high for the triggering using a microphone (see Figure 7a). Therefore, two strategies based on an electrical circuit which opens at specimen fracture. Figure 7b shows an electrical circuit using the embedded carbon fibers as electrical conductor. Copper contacts electrical connected to the carbon fiber ends form a closed loop that opens in case of specimen fracture leading to the triggering signal. By performing some tests, this method was found to be not reliable because some CFRP specimens did not break entirely, as a consequence, the electrical circuit still remained close. Moreover, this method is limited to unidirectional CFRP tested in fiber direction. Figure 7c presents the most reliable triggering method for CFRP. A conductive silver lacquer is painted on the surface of the specimens. As in the previous methods, two cables were applied on each end of the sample enabling a closed electrical circuit. Tests revealed that due to the shock wave that moves through the specimens after fracture spalling of the silver lacquer can be observed.

Results and discussion

Quasistatic tensile behavior. Figure 8 plots the experimental result of quasi-static tensile tests for wood in different grain orientations in a nominal stress-total strain diagram.

The axial tensile strength of beech wood, which corresponds to an angle of 0° relative to the fiber orientation, results in 113 MPa, while the strength of timber in an angle of 45° to the fiber orientation results in a significantly lower tensile strength of 12 MPa, the corresponding sample with an angle of 90° fail at 7 MPa. In terms of elongations, the specimen with 90° fiber direction shows the highest elongation of 1.9 % followed by 45° with 1.5 % and 0° grain orientation shows an elongation of 1.3 %. Fracture in all categories occurs abruptly without any visible signs of deformation. The measured brittle and anisotropic characteristics correspond to the known material behavior of wood reported in the literature.

The experimental results for vulcanized fiber in different rolling directions are plotted in Figure 9. The axial tensile strength of the 0° specimen is 57 MPa. This corresponds to 50 % of the tensile strength of the tested beech wood with corresponding angle. The 45° specimen of vulcanized fiber has a tensile strength of 85 % relative to the 0° specimens. The tensile strength of the 90° specimens is 68 % of the 0° specimens. This reveals that vulcanized fiber composite shows an anisotropic behavior but the dependence of the tensile strength to the rolling orientation is not as significant as the dependence of the tensile strength to the grain orientation of wood.

In the case of wood, no sign of deformation was visible before fracture. Vulcanized fiber shows a linear-elastic deformation behavior until reaching the yield stress σ_y. After that plastic deformation occurs. Therefore, the elongation of 11 % for 0° vulcanized fiber, 13 % for 45° and 12 % for 90° is in the order of 10 higher as compared to wood. Stress is still increasing in a linear behavior until it reaches its maximum, the ultimate stress σ_{ut}.

In the case of CFRP (see Figure 10), the nominal stress increases nearly proportionally with the total strain until fracture at a total strain of 1.7 % and a tensile strength of 2,300 MPa occurs.

As described in literature, the tensile strength is several times that of wood (20 times) and of vulcanized fiber (40 times). It shows a highly brittle characteristic with almost no distortion until fracture.

Fracture behavior captured by high-speed imaging. Figure 11 shows images from a 0° beech wood tensile test captured by 0.25 Mfps. The images show that a crack initialized on the right edge in the middle of the specimen. Then the crack developed along the grain to proceed longitudinal splitting which caused failure.

A different crack growth can be seen from Figure 12 which shows images from the fracture of 45° beech wood. The crack initialized in the middle from the left edge. Then the crack grew within 88 µs to the left edge. This led to a crack rate of 136 m/s. The crack propagated along the grain in an angle of approx. 45°.

Beech wood loaded perpendicular to the grains shows a similar behavior besides an angle of the crack propagation of 90°. Vulcanized fiber shows a crack propagation similar to the 90° beech wood (see Figure 13). Here the crack started from the upper left edge of the specimen and propagated perpendicular

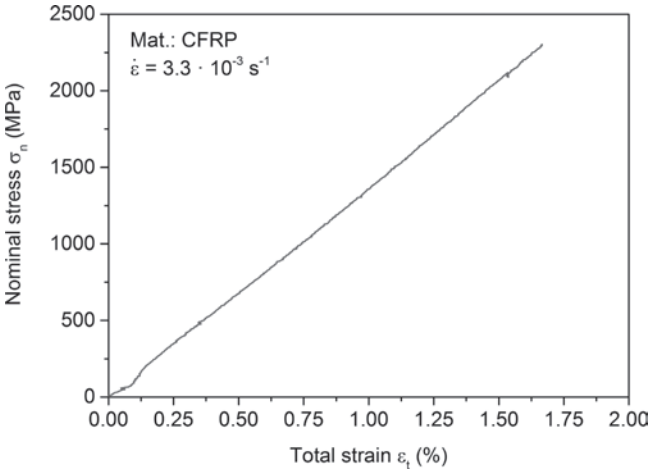

Figure 10: Nominal stress-total strain diagram of CFRP

to the loading direction to the opposite edge. This fracture took about 100 µs. Therefore, the fracture speed is with 100 m/s in the same order of magnitude as 45° beech wood.

Unlike wood, vulcanized fibers show no difference of fracture behavior in relation to their orientation. For vulcanized fibers and even more significantly for wood, an oscillation of the specimens after fracture could be identified. This is supposed to be the effect of elastical rebounding. The images in Figure 13 are also captured by a frame rate of 0.25 Mfps.

Figure 14 shows images of the fracture process of CFRP. To identify the fracture behavior, a frame rate of 2 Mfps is necessary.

The crack initialized from the upper left edge. Here first of all a small bundle of fibers excoriated. The full load had to be carried by the remaining fibers. This led to a sudden fracture at the mentioned localization. Therefore the crack propagation was also estimated. Afterwards the fractured specimen half rebounded. This led to compression of the remaining CFRP material. Due to the fact that CFRP is prone to compression, it came to a secondary fracture in the middle section of the specimen.

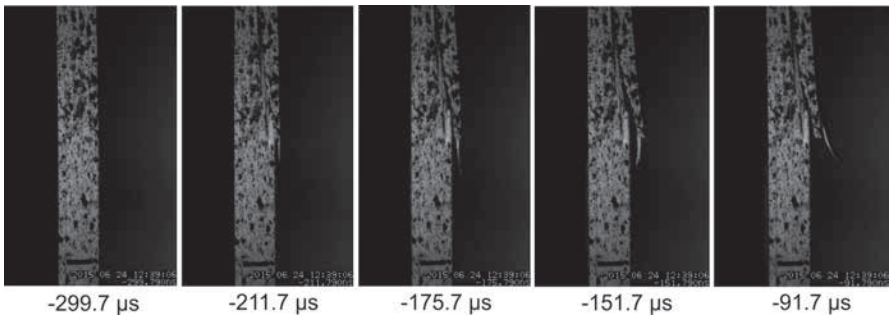

Figure 11: Fracture of 0° wood (frame rate: 0.25 Mfps, time stamps are relative time from trigger input)

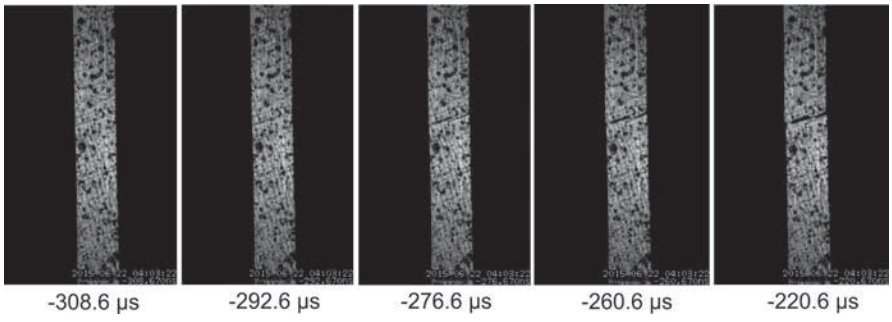

Figure 12: Fracture of 45° wood (frame rate: 0.25 Mfps, time stamps are relative time from trigger input)

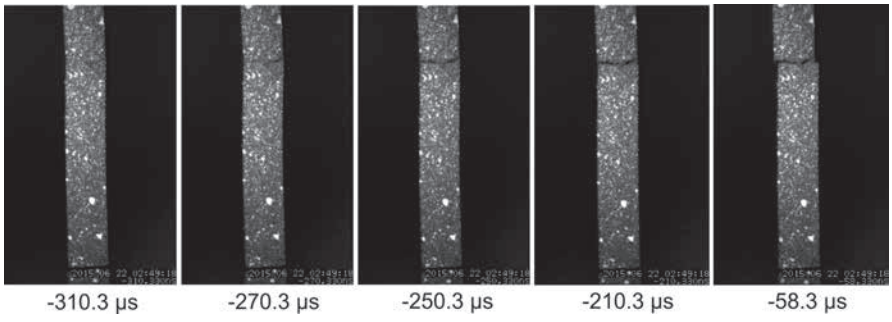

Figure 13: Fracture of 0° vulcanized fiber (frame rate: 0.25 Mfps, time stamps are relative time from trigger input)

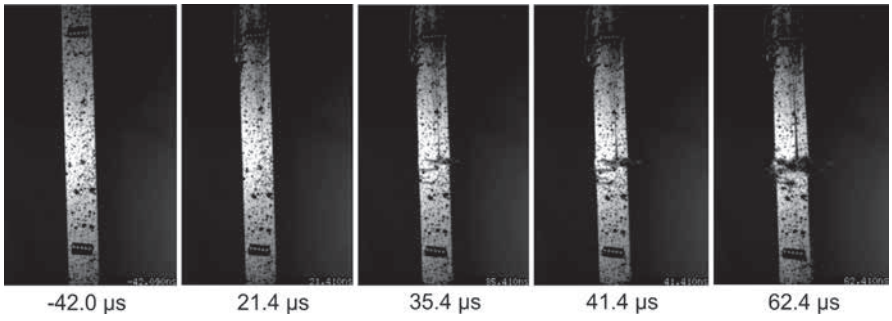

Figure 14: Fracture of CFRP (frame rate: 2 Mfps, time stamps are relative time from trigger input)

Strain distribution for high-speed images. The specimen strain distributions can be visualized by DIC for 0° wood as shown in Figure 15. Here the strain distribution helps to understand the fracture mechanism. For this sample, the crack initialized on the upper left edge and propagated diagonally to the lower right edge. Thereby, the maximum strain can be seen at the point of crack initiation. The surrounding of the crack remained nearly without a significant strain increase.

At this point it must be noted that the measured strain must be seen from the initial state right before fracture. An additional strain of approx. 1 % in average according to Figure 8 must be added.

An example for CFRP is given in Figure 16. The strain distribution at initial state was evenly distributed. The first sign of fracture was a first breakage of a small bundle of fibers at the upper right edge that was announced by a positive strain peak at this point. Afterwards the crack propagated from the left to the right edge. The remaining material below the crack propagation rebounded, which led to compressive strain. After total fracture the compressive strain increased until secondary fractures occurred. In the last image an uneven strain distribution is visible. It is assumed that local parts of the applied speckle pattern dissolved due to the change in strain. Therefore, some local points could even show positive strain peaks.

Due to the strain distribution, the crack propagation can be estimated more precisely than in Figure 14. Here the crack grew within 47.4 µs from one edge to the other. This led to a crack rate of 316 m/s.

Acoustic signals of high-frequency impulse measurements. The measured acoustic emissions are displayed in Figure 17 for wood and vulcanized fiber in each case for 0°, 45° and 90° orientation in form of process topographies that are showing the moment of fracture. The process topographies measured by HFIM are represented by the amplitude and frequency over time. For 0° wood amplitudes over the whole frequency spectrum were measured. 45° wood shows just in approx. 20 % of the frequency spectra amplitudes. The topography of 90° wood is marginally less as compared to 90° wood. For 0° vulcanized fiber the range of

frequency spectra is about 30 % of the frequency spectrum. 45° vulcanized fiber shows a significant reduction of the frequency range. The 90° vulcanized fiber shows the same frequency spectrum compared to 45° vulcanized fiber but marginal lower amplitudes. It is obvious that the reduction of the frequency range from 0° wood to the other wood orientation is not as distinctive as for 0° vulcanized fiber in comparison to other vulcanized fiber orientations. The topography of CFRP is not displayed because just one fiber orientation was investigated. It shows amplitudes over the whole measured frequency spectrum with higher amplitudes as that of 0° wood. In general, the order of distinction of the topography for each investigated material reflects well the tensile strengths.

Summary

High-speed imaging using advanced FTC-MOS sensors is suitable to visualize the fracture process from crack initiation to total fracture for beech wood and vulcanized fiber in different orientations and unidirectional carbon fiber-reinforced plastics (CFRP) tested in fiber direction under tensile loading. For wood and vulcanized fiber a frame rate of 0.25 Mfps is sufficient to record the whole fracture mechanism. For the faster crack propagation in CFRP 2.0 Mfps are required. Triggering for wood and vulcanized fiber using an acoustical microphone is the simplest and most reliable possibility. For CFRP a conductive silver lacquer applied to the surface of the specimen that opens an electrical circuit in the moment of fracture is the most reliable triggering method. The temperature increase due to the high light intensity could be reduced to 20 K by using a fan and a compressed air hose simultaneously for cooling. DIC technology can be used in combination with high-speed imaging by just adding a speckle pattern to the specimens and using the high-speed images for strain field calculations. Therewith fracture behavior can be investigated in more detail. High-frequency impulse measurement (HFIM) is able to visualize the acoustic energy release due to fracture. The tensile strength corresponds to the maximum process topography and frequency of HFIM.

Outlook

The presented results provide the basis for further studies, e. g., the investigations with higher strain rates and different temperatures. Moreover, other materials as well as different structures and orientations as well as different types of joints can be investigated by the described test setup to extend their range of applications. Improvements in the illumination techniques could lead to a further reduction of the temperature influence. High-speed camera technique could be even improved in the way of the image quality due to higher light sensitivity. At least, it is possible to use 3D-DIC with two high-speed camera systems for more complex geometries. The obtained data could be used for numerical investigations of fracture mechanisms.

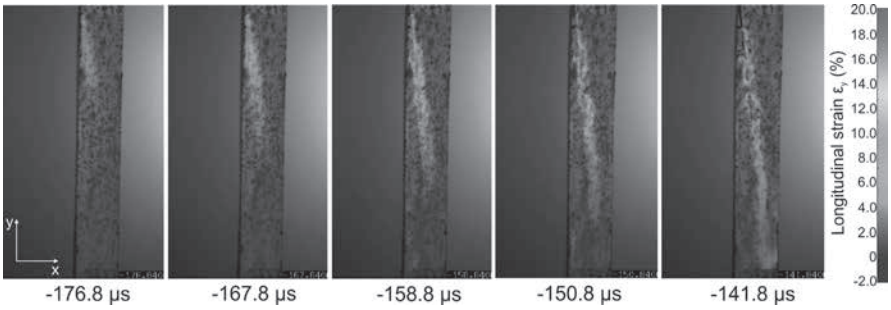

Figure 15: Fracture map of strain in load direction for 0° wood with DIC (frame rate: 0.25 Mfps, time stamps are relative time from trigger input)

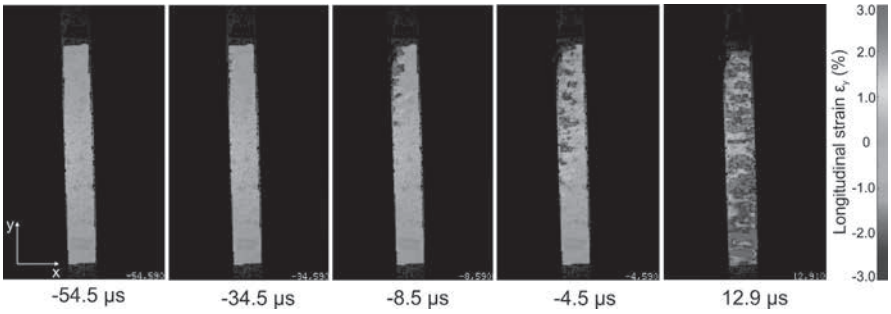

Figure 16: Fracture map of strain in load direction for CFRP (frame rate: 2 Mfps, time stamps are relative time from trigger input)

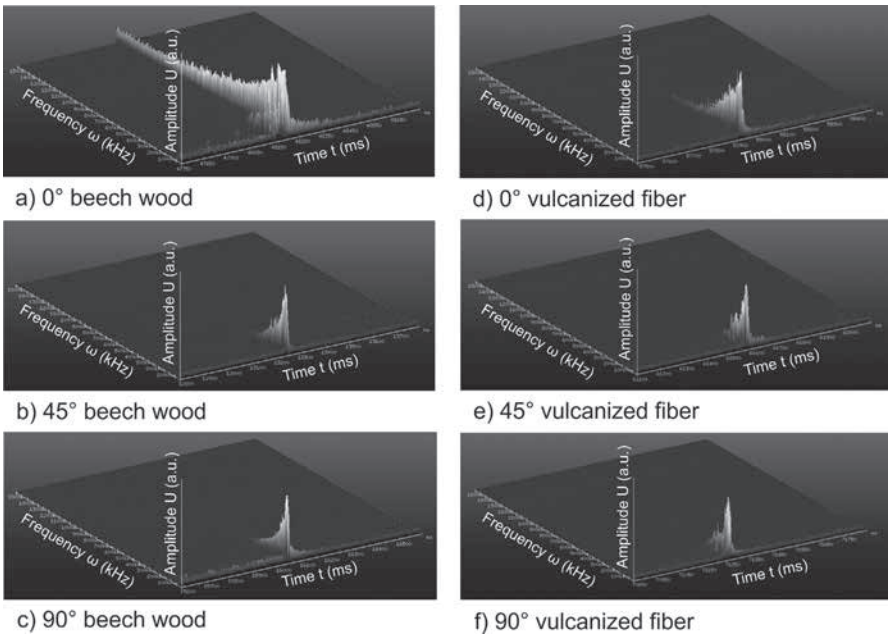

Figure 17: Process topography of high-frequency impulse measurements (HFIM) for beech wood and vulcanized fiber in different orientations

Acknowledgements

This research was supported by the Forschungsvereinigung Internationaler Verein für Technische Holzfragen e.V. – iVTH within the scope of the research program IGF-18266 N funded by the German Federal Ministry for Economic Affairs and Energy. Additionally, the authors would like to thank Mr. Lichtenberger from LIMESS Messtechnik und Software GmbH and Dantec Dynamics GmbH for their support for the DIC measurements.

References

1 D. Kohl, T. Flohr, S. Böhm: Adhesively bonded wood-based multi-material systems as a sustainable material for technical applications, Proc. of the 37th Annual Meeting of the Adhesion Society, San Diego, USA (2014), pp. 119-121
2 B. Penning, F. Walther, D. Dumke, B. Künne: Einfluss der Verformungsgeschwindigkeit und des Feuchtegehaltes auf das quasistatische Verformungsverhalten technischer Vulkanfiber, Materials Testing 55 (2013), No. 4, pp. 276-284 DOI:10.3139/120.110435
3 M. Kashfuddoja, M. Ramji: Whole-field strain analysis and damage assessment of adhesively bonded patch repair of CFRP laminates using 3D-DIC and FEA, Composites Part B 53 (2013), pp. 46-61
4 H. Kusano, Y. Aoki, Y. Hirano, T. Hasegawa, Y. Nagao: Visualization on static tensile test for unidirectional CFRP ,17th International Conference on Composite Materials ICCM-17 (2009), http://www.iccm-central.org/Proceedings/ICCM17proceedings/Themes/Behaviour/DEFORM%20%26%20FRACTURE%20OF%20COMP/INT%20-%20DFC/IF8.2%20Kusano.pdf (01.10.2015)
5 Y. Kondo, K. Takubo, H. Tominags, R. Hirose, N. Tokuoka, Y. Kawaguchi, Y. Takaie, A. Ozaki, S. Nakaya, F. Yano, T. Daigen: Development of "HyperVision HPV-X" High-speed Video Camera, Shimadzu Review 69 (2012), pp. 285-291, http://www.shimadzu.com/an/journal/selection/SR13_002E.pdf (01.10.2015)
6 H. Kusano, T. Mizuno, A. Yamada, Y. Aoki, Y. Hirano: High resolution measurement for fracture behavior observations of CFRP, 18th International Conference on Composite Materials (2011), http://www.iccm-central.org/Proceedings/ICCM18proceedings/data/2.%20Oral%20Presentation/Aug23%28Tuesday%29/T32%20Impact%20and%20Dynamic%20Response/T32-6-AF1475.pdf (01.10.2015)
7 S. A. Krishnana, A. Baranwalb, A. Moitraa, G. Sasikalaa, S. K. Alberta, A. K. Bhaduria, G. A. Harmainb, T. Jayakumara, E. Rajendra Kumarc: Assessment of deformation field during high strain rate tensile tests of RAFM steel using DIC technique, Procedia Engineering 86 (2014), pp. 131-138 DOI:10.1016/j.proeng.2014.11.021
8 J. Qin, R. Chen, X. Wen, Y. Lin, M. Liang, F. Lu: Mechanical behaviour of dual-phase high-strength steel under high strain rate tensile loading, Materials Science & Engineering A 586 (2013), pp. 62-70 DOI:10.1016/j.msea.2013.07.091
9 T. Brynk, A. Laptiev, O. Tolochyn, Z. Pakiela: The method of fracture toughness measurement of brittle materials by means of high-speed camera and DIC, Computational Materials Science 64 (2012), pp. 221-224 DOI:10.1016/j.commatsci.2012.05.025
10 D. Hülsbusch, F. Walther: Damage detection and fatigue strength estimation of carbon fibre reinforced polymers (CFRP) using combined electrical and high-frequency impulse measurements, The e-Journal of Nondestructive Testing 20 (2015), No. 1, pp. 1-9
11 U. Karrenberg: Signale-Prozesse-Systeme – Eine multimediale und interaktive Einführung in die Signalverarbeitung, Springer Verlag, Heidelberg, Germany (2010)

Abstract

Hochpräzisionsbestimmung der Verformungs- und Schädigungsentwicklung von Verbundwerkstoffen mittels Hochgeschwindigkeitskamera sowie Hochfrequenzimpulsmessung und digitaler Bildkorrelation. Verbundwerkstoffe wie Holz, Vulkanfiber und kohlenstofffaserverstärkter Kunststoff (CFK) sind hinsichtlich ihrer mechanischen Eigenschaften bereits charakterisiert, allerdings fehlen bisher detaillierte Informationen zu den Bruchmechanismen und zum Verformungsverhalten unmittelbar vor dem Bruch. Für CFK liegt dies u.a. in der sehr hohen Bruchgeschwindigkeit begründet. Kenntnisse über die Schädigungsentwicklung beim Rissbeginn und -fortschritt können jedoch dabei helfen, die Empfindlichkeit und den Widerstand gegenüber Brüchen durch eine optimierte Materialstruktur zu verbessern und diese Materialien für strukturelle Anwendungen weiter zu qualifizieren. Da für die untersuchte Werkstoffgruppe die Bruchmechanismen bisher mit konventioneller Messtechnik nicht hinreichend genau detektiert werden konnten, wird in dieser Arbeit die simultane Anwendung innovativer Messtechniken vorgestellt, um diese Lücke zu schließen. Das Bruchverhalten in Zugversuchen wurde mittels eines Hochgeschwindigkeitskamerasystems aufgenommen, dessen Informationen zur Visualisierung mittels digitaler Bildkorrelation (DIC) ausgewertet wurden. Gleichzeitig wurde durch Einsatz der Hochfrequenzimpulsmessung (HFIM) das Spektrum mechanischer Schwingungen ermittelt, das zuverlässige Informationen über freigesetzte Energien liefert. Die Herausforderung einer geeigneten Triggerung der Hochgeschwindigkeitskamera wurde materialspezifisch gelöst. Durch die Verwendung von Hochleistungs-Lichtquellen wurde eine Aufnahmegeschwindigkeit von 2 Millionen Bildern pro Sekunde erreicht. Die Untersuchungen liefern detaillierte Informationen über die unterschiedlichen Bruchmechanismen, wobei Holz und Vulkanfiber aufgrund ihrer Anisotropie in verschiedenen Orientierungen charakterisiert wurden.

Bibliography

DOI 10.3139/120.110813
Materials Testing
57 (2015) 11-12, pages 933-941

ISSN 0025-5300

The authors of this contribution

Dipl.-Wirt.-Ing. Sebastian Myslicki, born in 1982, studied Industrial Engineering with specialization in Production Management at TU Dortmund University, Germany. After his diploma thesis, he has been working as a scientific assistant at Materials Test Engineering (WPT) in the Faculty of Mechanical Engineering of TU Dortmund University, Ger-

many, headed by Prof. Walther. His research focus is on fatigue and fracture of composite materials.

Dr. Markus Ortlieb finished his PhD in the Department of Physical Chemistry, Ruhr University Bochum, Germany, in the field of laser spectroscopy and laser microscopy in 2008. He is currently working at Shimadzu Europe GmbH as a trainer and developer in the product marketing group and supports applications in the field of material testing and spectroscopy.

Dipl.-Phys. Gerrit Frieling studied Physics at RWTH Aachen University, Germany. He is working as a scientific assistant at Materials Test Engineering (WPT) in the Faculty of Mechanical Engineering of TU Dortmund University, Germany.

Prof. Dr.-Ing. Frank Walther, born in 1970, studied Mechanical Engineering majoring in Materials Science and Engineering at TU Kaiserslautern University, Germany, from 1992 to 1997. There he finished his PhD on the fatigue assessment of highly-loaded railway wheel steels at the Institute of Materials Science and Engineering (WKK) in 2002. From 2002 to 2008, he headed the research group Fatigue Behaviour at WKK and finished his postdoctoral qualification (habilitation) in Materials Science and Engineering in 2007. Afterwards, he joined Schaeffler AG in Herzogenaurach, Germany, and took responsibility for Public Private Partnership comprising public research funding and materials research projects within corporate development. Since 2010, he has been Professor for Materials Test Engineering (WPT) at TU Dortmund University, Germany. His research portfolio includes determination of structure-property relationships of metal- and polymer-based materials and components taking the influence of manufacturing and joining processes as well as service loading and corrosion deterioration into account. New measurement and destructive/nondestructive testing techniques are applied for the characterization of fatigue behavior from LCF to VHCF range under mechanical, thermal, chemical and mixed influences, as well as new physically-based approaches for the calculation of damage development and (remaining) fatigue life. Besides, he is engaged in various committees, e. g., as referee for the German Research Foundation (DFG), member of Board of German Materials Society (DGM), member of German Association for Materials Research and Testing (DVM), member of Board of Association of German Engineers (VDI) and member of Scientific Association of Materials Engineering (WAW). He has published more than 130 reviewed papers and conference proceedings so far and maintains close scientific contact with institutions and industries in materials science and engineering field worldwide.